Available online at www.sciencedirect.com
ScienceDirect
Advances in Space Research 45 (2010) 183–199
ADVANCES IN SPACE RESEARCH (a COSPAR publication)
www.elsevier.com/locate/asr

A mars communication constellation for human exploration and network science

Francesco Castellini [a,*], Andrea Simonetto [b], Roberto Martini [a], Michèle Lavagna [a]

[a] Aerospace Engineering Department, Politecnico di Milano, Via La Masa 34, 20156 Milano, Italy
[b] Delft Center for Systems and Control, TUDelft, Mekelweg 2, 2628 CD Delft, The Netherlands

Received 19 September 2008; received in revised form 18 October 2009; accepted 23 October 2009

Abstract

This paper analyses the possibility of exploiting a small spacecrafts constellation around Mars to ensure a complete and continuous coverage of the planet, for the purpose of supporting future human and robotic operations and taking advantage of optical transmission techniques. The study foresees such a communications mission to be implemented at least after 2020 and a high data-rate requirement is imposed for the return of huge scientific data from massive robotic exploration or to allow video transmissions from a possible human outpost.

In addition, the set-up of a communication constellation around Mars would give the opportunity of exploiting this multi-platform infrastructure to perform network science, that would largely increase our knowledge of the planet.

The paper covers all technical aspects of a feasibility study performed for the primary communications mission. Results are presented for the system trade-offs, including communication architecture, constellation configuration and transfer strategy, and the mission analysis optimization, performed through the application of a multi-objective genetic algorithm to two models of increasing difficulty for the low-thrust trajectory definition.

The resulting communication architecture is quite complex and includes six 530 kg spacecrafts on two different orbital planes, plus one redundant unit per plane, that ensure complete coverage of the planet's surface; communications between the satellites and Earth are achieved through optical links, that allow lower mass and power consumption with respect to traditional radio-frequency technology, while inter-satellite links and spacecrafts-to-Mars connections are ensured by radio transmissions. The resulting data-rates for Earth–Mars uplink and downlink, satellite-to-satellite and satellite-to-surface are respectively 13.7 Mbps, 10.2 Mbps, 4.8 Mbps and 4.3 Mbps, in worst-case.

Two electric propulsion modules are foreseen, to be placed on a $C_3 \sim 0$ escape orbit with two Zenith Sea Launch rockets in March 2021 and carrying four satellites each. After the entrance in Mars sphere of influence, the single spacecrafts separate and spiral-down with Hall effect thrusters until they reach the final operational orbits in April 2025, at 17,030 km of altitude and 37 deg of inclination. The preliminary design includes 105 kg and 577 W of mass and power margin for each satellite, that can be allocated for scientific payloads.

The main challenges of the proposed design are represented by the optical technology development and the connected strict pointing constraints satisfaction, as well as by the Martian constellation operations management.

This mission study has therefore shown the possibility of deploying an effective communication infrastructure in Mars orbit employing a small amount of the resources needed for the human exploration programme, additionally providing the chance of performing important scientific research either from orbit or with a network of small rovers carried on-board and deployed on the surface.

Keywords: Mars constellation; Laser communications; Low-thrust trajectory optimization; System level design; Network science

* Corresponding author. Tel.: +39 059221792.
E-mail addresses: castellfr@gmail.com, castellini@aero.polimi.it (F. Castellini), a.simonetto@tudelft.nl (A. Simonetto), robertomartini5@virgilio.it (R. Martini), lavagna@aero.polimi.it (M. Lavagna).

0273-1177/$36.00 © 2009 COSPAR. Published by Elsevier Ltd. All rights reserved.
doi:10.1016/j.asr.2009.10.019

1. Introduction

Mars is the primary long term target of all space exploration programs, and a massive robotic endeavour is foreseen for the near future, with efforts from different space agencies possibly leading to an international Mars Sample Return (MSR) mission in the 2020 timeframe and to a first human mission around 2030.

The current Earth–Mars communication infrastructure consists of three orbiters, NASA's Mars Odyssey and Mars Reconnaissance Orbiter (MRO) and ESA's Mars Express, occasionally working as relays from the surface. Data about these spacecrafts are presented in Table 1, where the now concluded Mars Global Surveyor (MGS) mission is also included; MRO was specifically designed to act also as a communication link between NASA rovers and Earth, and carries a technology demonstrator of Ka transmission band, that allows higher data-rate with lower power. For this purpose, note the progression towards higher frequencies and thus higher data-rates in the communication link, that would have culminated in 2009 in an optical connection technology demonstrator on-board the now cancelled NASA Mars Telecom Orbiter.

The current best data-rate is of about 500 Kbps in worst-case Earth–Mars distance, but this is achievable only with the massive and powerful MRO. In light of the progressively increasing amount of scientific data to be returned to Earth, such a performance could become inadequate; moreover, in order to allow human exploration, continuous highly reliable and high data-rate communications must be previously ensured.

In this scenario, the paper presents a feasibility study carried out at Politecnico di Milano by a team of students for a mission with the primary objective of developing a feasible design solution for a communications constellation capable of continuously ensuring a data-rate of at least 500 Kbps and preferably higher from any point of Mars surface, with built-in multiple redundancies aimed at preventing from leaving the astronauts isolated on the surface. Although other studies exist regarding Martian constellations for both communications and navigation, the work described in this paper represents, to the authors knowledge, the first system design allowing to satisfy the requirement of high data-rate continuous and complete coverage of Mars surface. The requirement of the complete coverage of the planet comes from the current uncertainty in the location of the first human base, that is not likely to be resolved until the last phase of the human mission design process, and from the possible presence of a network of scientific outposts in the 2025–2035 timeframe. Particular attention has been paid to the global optimization of the system, in order to restrain the total cost of the mission and include it more easily in the larger Mars exploration context. During the study, launch dates have been considered in order to have the infrastructure operational around 2025, but it is unlikely that funding for such a precursor mission would be approved before a precise date has been set for the first human landing.

It has however to be noted that the launch of a constellation of satellites around Mars would also give the unique opportunity of having several orbiting platforms with the same characteristics, therefore very well suited for the deployment of a net of scientific payloads for the study of some aspects of the Red Planet that are still mostly unknown and for which multiple contemporary observation points are required, such as global circulation and climatological cycles.

The mission design process has been carried out without directly allocating resources for this secondary scientific objective, but results will be presented that show how the final margins for both mass and power would allow the re-design in later phases of some subsystems to include on-board science instruments.

The paper presents the proposed mission according to the following outline: Section 2 describes the system level trade-offs performed for the communication link, the constellation configuration and the transfer strategy, along with a brief mission outline, Section 3 reports the results of the mission analysis optimization, Section 4 presents a summary of the proposed subsystems design and Section 5 draws some final remarks and suggests few scientific opportunities to be further developed in later studies.

For more detailed information, the complete Feasibility Study Report (that will be indicated with FSR in this paper) is available at the web address http://publishing.yudu.com/Freedom/Anpja/MarsWebfeasibilityst or can be requested to the authors.

Table 1
Mars orbiters system and communication data summary (data between brackets for MTO mission are referred to the laser link payload).

	Mission name				
	MGS	Mars Odyssey	Mars Express	MRO	MTO
Launch year	1996	2001	2003	2005	2009
Life [years]	10	6	6	10	10
Wet mass [Kg]	1060	725	1200	2200	2500
Power [kW]	0.98	0.75	0.5	2	>1 (0.12)
Antenna [m]	1.5	<1.5	1.6	3	3 (30 cm)
RF Band	X	X	S/X	X/Ka	X/Ka
Data-rate [kbps]	25–85	30–124	28–182	500–3500	10,000–30,000
Technology	Aerobraking	Deployable antenna	–	Ka-band	Laser link
Cost [M$]	400	297	300	720	500

2. Mission trade-offs

When facing with the difficult task of developing a complex infrastructure for the complete and continuous coverage of Mars with the minimum possible amount of resources, many system level trade-offs arise that tremendously affect the final cost of the mission, especially for the definition of the communication technology and communication system architecture, of the number and orbital position of the spacecrafts, and of the transfer strategy to carry the satellites from Earth to the final operational orbits. The performed studies and the proposed solutions in these three fundamental areas are presented in the next paragraphs.

2.1. Communication link trade-off

To obtain the required data-rate, it is possible either to increase the capabilities of the distant spacecrafts communication system or to improve the sensitivities of the Earth reception systems. Indeed, both of these approaches have been used for deep space missions, but further increases are hard to accommodate. Current missions are in fact already flying large antennas with rather high power consumptions in relation to the far solar distance, and on the Earth end, NASA Deep Space Network (DSN) antennas are 34-m and 70-m diameters, with receiving system low-noise amplifiers already operating at a few degrees above absolute zero. More advances in conventional communications capabilities are planned, but the promise of a future jump in deep space communication systems comes from the much higher frequencies of the optical signals. Over the history of the DSN, conventional RF performance has improved about 12 orders-of-magnitude due to sustained research and development (R&D) efforts at JPL. The change from X-band (~8 GHz) to Ka-band (~32 GHz), demonstrated on-board MRO, has a theoretical improvement due to frequency squared of 11.6 dB, although practical factors (e.g., atmospheric losses) have limited that improvement to about 6 dB. The promise of optical communications is even more attractive, due to the jump in frequency to approximately 300,000 GHz. For this reason, substantial work has been performed in the past 10 years on the analysis of optical link systems, especially in light of the planned MTO mission, leading to numerous papers (Moision and Hamkins, 2003; Khaltri et al., 2004; Townes et al., 2004; Biswas and Piazzolla, 2003, 2005; Hemmati, 2005) and ESA Artemis mission has demonstrated the use of laser for communications in Earth orbit.

Though with the cancellation of MTO the concept of Earth–Mars laser communications will not be proved in the upcoming years, the current study is referred to a timeframe after the 2020, leaving plenty of time for the technology maturation. Considering a worst-case distance of 2.7 AU and a direct communication from a spacecraft around Mars towards a ground station on Earth, the results of Table 2 have been obtained by Hemmati et al. (1996 and 1997), clearly showing the definite advantages given by optical communications in terms both of mass and power. For this reason, in light of the goal of minimizing the required resources, an optical communication system has been preferred to the traditional RF architecture.

The wider problem of the selection of the number of platforms and their orbital position for the complete coverage of the planet and the continuous connection with Earth is addressed in the next paragraph.

2.2. Constellation trade-off and design

The following three different communication architectures have been evaluated for accomplishing the requirements of complete and continuous coverage of Mars surface:

- Two spacecrafts in Halo orbits near L_1 and L_2, as suggested by Strizzi et al. (2001). This option minimizes the number of required platforms (99.81% of coverage with only two spacecrafts), but the large distance, i.e. about 1 million km, between the surface and the Lagrangian points complicates the communications, and the failure of one satellite would leave half of the planet in complete black-out.
- Two spacecrafts in Halo orbits near L_1 and L_2 plus a constellation of small spacecrafts, e.g. with a lightweight design (less than 100 kg) similar to that proposed by Cesarone et al. (1999), to be used only as relays from the surface to the Lagrangian points, solving both the communication distance and redundancy issues. However, such an architecture presents severe tracking problems from the spacecrafts in the Lagrangian points to the constellation.
- A Mars constellation of satellites directly linked to Earth, without the exploitation of Lagrangian Points. Although this solution requires a high number (at least 6) of spacecrafts with high data-rate Earth–Mars communication capability to ensure the global coverage, it

Table 2
Comparison in mass and power requirements for optical and radiofrequency (X-band and Ka-band) link for Mars–Earth communications, according to Hemmati et al. (1996 and 1997).

Data volume [Gb/day]	Communication band	Mass [kg]	DC power [W]
0.1	X-band	10.1	18.9
	Ka-band	10.0	15.2
	Optical	6.4	19.9
1.0	X-band	12.0	40.0
	Ka-band	11.3	25.0
	Optical	7.4	22.8
10.0	X-band	22.7	104.9
	Ka-band	22.5	46.0
	Optical	12.1	44.6

allows to develop a unique and simple spacecrafts design, avoiding tracking problems and ensuring redundancy if a sufficient number of platforms is foreseen.

After more detailed analyses, the first two options have been discarded; as regards to the first option in fact, the redundancy requirement would impose the use of 4 spacecrafts in the Lagrangian points, massive enough to ensure high data-rate communications with Mars surface, either with a laser steering mechanism or with a large conventional antenna and powerful RF system; the second option on the other hand would imply the design and development of two different types of spacecrafts with complex mechanisms for the tracking of the constellation, thus leading to higher program costs that are not acceptable.

The third option has therefore been selected as baseline, with the implementation aboard each spacecraft of an optical communication device for Earth–Mars–Earth link. However, such instrument requires an extremely high pointing accuracy and a quiet vibration environment, thus imposing a three-axes stabilized spacecraft with the less moving mechanisms as possible. Hence, the designed optical communication system does not employ mechanical gimbals as laser pointing device; beam steering is instead accomplished by actuation of the optical train, ensuring the required accuracy without strongly affecting neither the vibration environment nor the spacecraft's mass budget. As a drawback, such actuation only allows for small angular displacements from the reference pointing given by the spacecraft attitude; hence, the use of two lasers for contemporarily communicating with two targets is prevented, unless their relative geometry is fixed in time, which is not the case for the most interesting links, as for example Earth and Mars surface, or Earth and another spacecraft of the constellation.

These constraints have led to a complex communication architecture composed of two orbital planes separated of 180° in Right Ascension of Ascending Node (RAAN) with three operational satellites each, as shown in Fig. 1. Each satellite has three relatively fixed but rotating RF antennas to communicate with the other satellites and with Mars soil. The central antenna has to ensure the largest possible coverage of the planet in order to limit the number of required orbital platforms and avoid the need of tracking single elements on the surface, hence an X-band antenna has been selected, having a larger beamwidth angle (approximately 20°) with respect to Ka-band. This directly leads to the choice of the constellation height of 17,030 km, which represents the minimum altitude allowing to include in the X-band beam the entire planet. For the other two antennas, since the architecture of the constellation is well defined a narrow beamwidth can be exploited, leading to the choice of Ka-band. The inter-satellite link has the dual purposes of allowing to beam back to Earth information collected by a satellite positioned behind Mars and of ensuring a *first level of redundancy* to the system; if a laser fails in fact, the satellite can still receive data from the surface contributing to the global coverage of the planet and communicating with Earth through the other two satellites of its orbital plane. A drawback of this approach is the need of a 3-degrees of freedom (DoF) mechanisms for the movement of the antennas, that are fixed with respect to each other but have to continuously point towards the nadir while the spacecraft is an inertial three-axis stabilized Earth pointer for the laser communication with the ground stations.

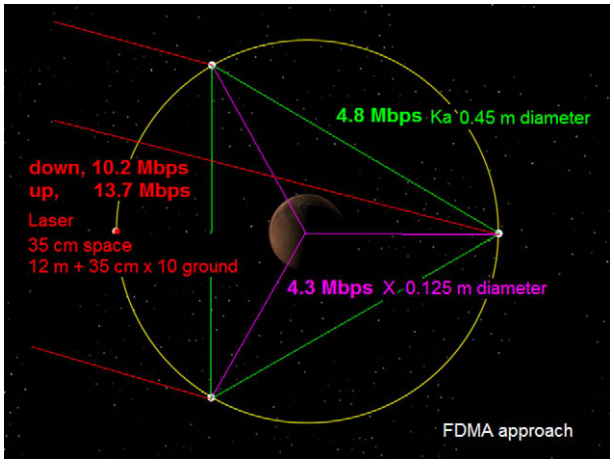

Fig. 1. Communication architecture layout, showing one of two orbital planes and main communication data-rates.

For the constellation design, in addition to the constraints given by the communication architecture (three satellites per orbital plane, 180° RAAN separation, circular orbits at 17,030 km of altitude, that coincidentally corresponds to the Mars stationary altitude), the same inclination for both planes has been imposed, in order to have the same J_2 effect on the RAAN, and therefore maintaining fixed at the first order of approximation the constellation geometry, allowing a low propellant consumption for station keeping.

A Walker $T/P/F$ constellation has thus been selected, where $T = 6$ is the total number of satellites, and $P = 2$ is the number of orbital planes, with two free parameters to be exploited as optimization variables: the constellation inclination and the phase shift $\Delta\theta = F360/T$ between the satellites of the two orbital planes. Two main optimization objectives have been considered, global coverage and coverage of the equatorial zones, in light of the higher probability of such a location for the first human base. Considering the optimal $\Delta\theta$ for each inclination and simulating the planet coverage during one orbit of the satellites (equal to 1 Sol), Fig. 2 shows the global uncoverage percentage, computed as in Eq. (1) where $N_{\mathrm{TimeIntervals}}$ is the number of time intervals in which the simulation time is divided and N_{GRIDS} is the number of latitude–longitude boxes covering the surface.

$$\text{Global uncoverage percentage} = \frac{\sum_{i=1}^{N_{TimeIntervals}} \text{Number of uncovered grids at time} i}{N_{TimeIntervals} \cdot N_{GRIDS}} \quad (1)$$

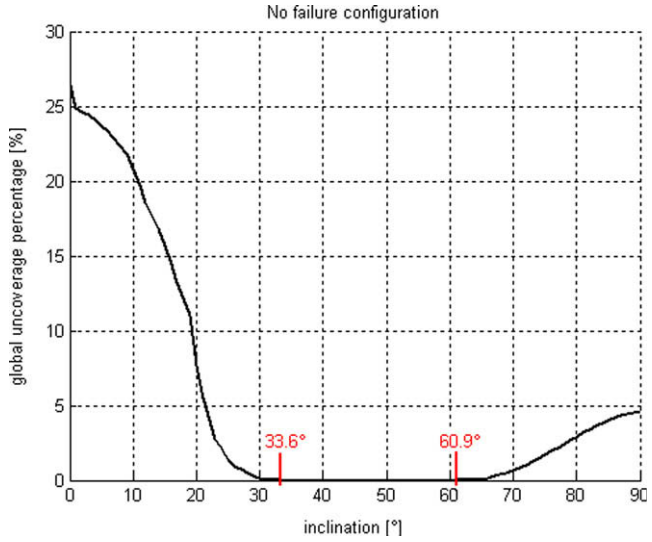

Fig. 2. Global uncoverage index as a function of the inclination of the orbital planes, with optimal phase shift for each inclination and no failure configuration.

With the mentioned constraints, a large inclination band from 33.6° to 60.9° ensures the complete and continuous coverage of the planet as requested; the 1-failure configuration has therefore been analyzed, and the results in Fig. 3 show that the optimal inclination for the global coverage is around 60°. However, $i = 37°$ has been chosen, being the maximum inclination ensuring the complete coverage of the equatorial ±20° latitude band even in a 1-failure scenario, which can be considered a second level of redundancy.

An optimal phase shift $\Delta\theta = 5°$ has been found for $i = 37°$, defining a Walker 6/2/0.083 constellation. The performances for the 1-failure configuration are summarized in Fig. 4, showing a worst-case maximum revisit time of

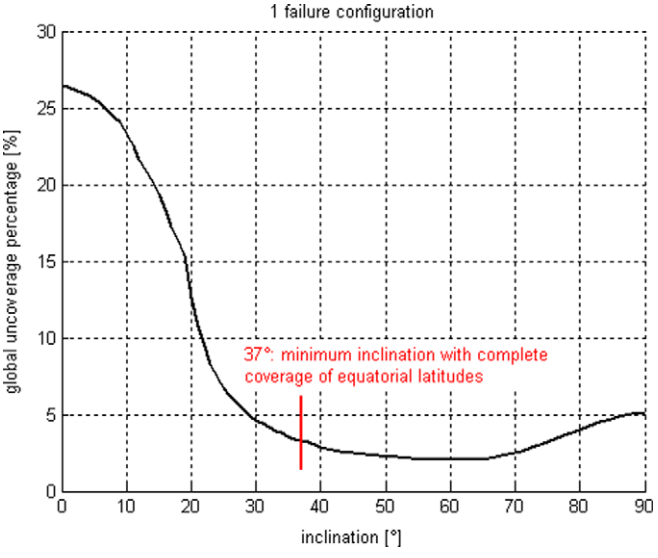

Fig. 3. Global uncoverage index as a function of the inclination of the orbital planes, with optimal phase shift for each inclination and 1-failure configuration.

about 9.1 h at 61° of latitude. The gap zone, whose longitude depends on the failed satellite, moves in time towards west due to J2 effect, eventually returning in the same longitudinal position after about 52 years. With the contemporary failure of two spacecrafts, the performances of the constellation become unacceptable, with a wide area near the equator never communicating with Earth. For this reason and to take into account the unlikely case that a human base is set-up in the latitude–longitude box with degraded performances, a spare strategy has been developed as *third level of redundancy*, including one dormant satellite for each orbital plane for the replacement of any failed satellite in its plane. After repositioning the spare spacecraft, the complete coverage of the equatorial band is ensured even with two failed satellites on the same orbital plane, with good revisit times over the entire planet shown in Fig. 4.

Summarizing, the chosen communication architecture and constellation configuration has the following advantages: (1) continuous and complete coverage of the planet, (2) high data-rate with low mass systems, (3) readiness, since it does not need ground tracking, (4) three levels of redundancy, with the minor disadvantages of the 3-DoF antennas mechanism and of the communication systems complexity.

As a final remark, it has to be noted that one key issue not solved with the proposed mission architecture is the Solar conjunction problem: every 2.19 years, the Sun is located between Earth and Mars and the communications between the two planets are interrupted. Over a time span of 10 years from 2025 to 2035 and considering a conservative value of 3° for the minimum Earth–Mars–Sun angle that allows communications, the black-out periods last from 8 to 23 days depending on Mars distance from the node line of its orbit. However, as shown by Morabito and Hastrup (2001), low data-rate in Ka-band communications could be possible until 0.65° of Earth–Mars–Sun angle, considerably reducing the black-out times (with one black-out lasting 4 days in 2030 and none during the other conjunctions). However, the only way to fully solve the solar conjunction issue is to design a relay satellite to be placed in a heliocentric orbit with continuous Earth and Mars visibility during the Solar conjunction periods, as proposed for example by Gangale et al. (2008); since this spacecraft would act as Earth–Mars relay point only for a very limited amount of its lifetime, a primary scientific mission would have to be defined in order to justify its development.

2.3. Transfer strategy trade-off and mission outline

In the frame of a Mars mission, many different transfer strategies are available, that strongly influence the final configuration's mass, power, dimensions and consequently cost; both chemical propulsion (CP) and electrical propulsion (EP) have advantages and disadvantages in terms of specific impulse, subsystems mass, time of flight and improvement prospects, hence a quantitative trade-off study has been performed to determine the optimal solu-

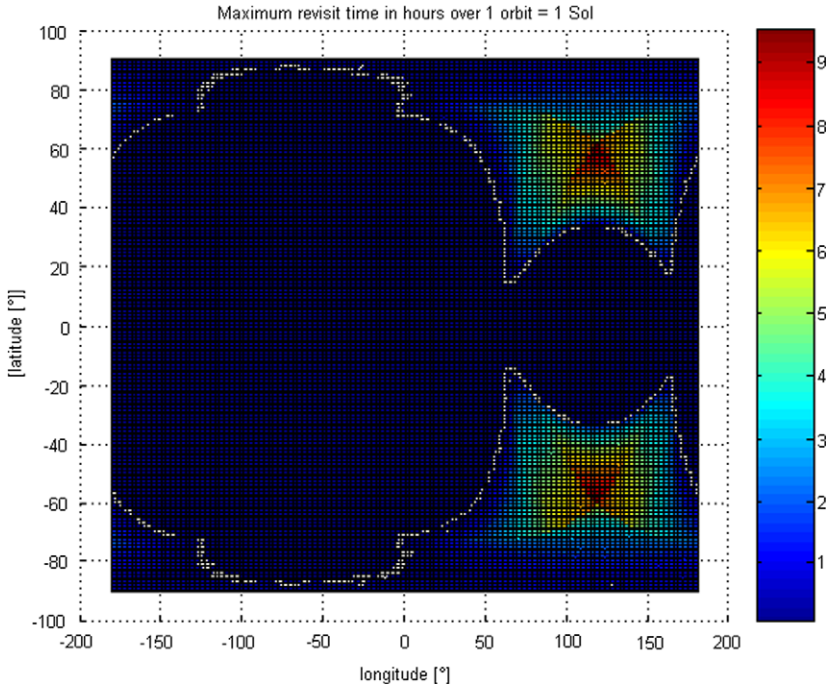

Fig. 4. Maximum revisit time over 1 Sol for the selected constellation, 1-failure configuration.

tion. The options summarized in Table 3 have been analyzed, including *trans*-Mars direct injection with the launcher, CP transfer from a Geostationary Transfer Orbit (GTO) and EP transfer from an escape trajectory. In the latter two cases, both separate transfers of the single spacecrafts and the use of propulsion modules carrying several spacecrafts have been considered. Similarly, Mars orbit insertion (MOI) can be obtained with CP, either with a single burn at the pericentre of the incoming hyperbolic trajectory or an aerobraking phase and a final circularization burn, or EP, with a slow spiral-in low-thrust phase. However, it is not feasible to use EP to capture the spacecraft in Mars orbit if the arrival velocity is high, therefore EP MOI has been considered only after EP transfer from Earth; the use of aerobraking for MOI has been instead foreseen only for CP Earth–Mars transfer, because the low incoming velocity resulting from EP transfer results in a lower ΔV with the direct MOI strategy.

To perform the trade-off, the dry mass of the single spacecraft excluding power and propulsion subsystems has been fixed for all options to 213 kg, including a 20% system level margin and coming from a preliminary mass budget based on a first-glance payload mass estimation (laser and RF communication hardware) and on the allocation for the other subsystems of mass percentages reflecting a database of recent Mars orbiters.

The C_3 energy provided by the launcher, the launch date, the time of flight (TOF) and additional guidance parameters for the low-thrust trajectories have then been exploited as degrees of freedom for the mission analysis optimization, presented in Section 3, that has returned the ΔV (and thus propellant mass) values for each option.

Table 3
Description of the 7 transfer strategy options analyzed for the quantitative trade-off.

Option	Earth–Mars transfer	Mars orbit insertion
1	Separated spacecrafts direct launcher injection	Separated spacecrafts, CP with aerobraking
2	CP module with 4 spacecrafts from GTO	Separated spacecrafts, CP with aerobraking
3	Separated spacecrafts, CP from GTO	Separated spacecrafts, CP with aerobraking
4	EP module with 4 spacecrafts from $C_3 = 0$	Separated spacecrafts, CP with aerobraking
5	EP module with 4 spacecrafts from $C_3 = 0$	EP MOI with the same transfer module engines
6	EP module with 4 spacecrafts from $C_3 = 0$	Separated spacecrafts, EP MOI
7	Separated spacecrafts, EP from $C_3 = 0$	Separated spacecrafts, EP MOI

Propulsion and power subsystems have been sized on the basis of the required thrust, V and power for each considered transfer option, using simplified relations and a database of engines and power generation and distribution components; a guesstimated power need of 500 W for the spacecraft during its lifetime has been added to the power request given by the electrical engines. For the options involving a propulsion bus carrying the satellites, its propulsion and power masses have been similarly computed, and the bus structural mass has been estimated through compression buckling, tensile strength and natural frequencies sizing.

Table 4
Quantitative trade-off results for the 7 analyzed options. In bold: selected option; in italics: options discarded for lack of launch redundancy; underlined: options discarded for operational complexity issues.

Transfer strategy option & number of launches	Launch orbit	Total launch mass (excluded adapters)	Candidate launcher(s) and mass margin
Option 1, 1 launch	*Direct injection*	*6517 kg*	*Delta IV (7%)*
Option 1, 2 launches	Direct injection	3258 kg	Proton M Breeze (28%)
Option 2, 1 launch	*GTO*	*9348* kg	*Ariane 5 ECA (7%)*
Option 2, 2 launches	GTO	4719 kg	Proton M Breeze (9%) H II LRB (21%)
Option 3, 1 launch	*GTO*	*9265 kg*	*Ariane 5 ECA (8%)*
Option 3, 2 launches	GTO	4632 kg	Proton M Breeze (11%) H II LRB (23%)
Option 4, 2 launches	$C_3 = 0\ km^2/s^2$	3725 kg	Delta II (2%) Zenit 3 SL (7%)
Option 5, 2 launches	$C_3 = 0\ km^2/s^2$	3649 kg	Delta II (4%) Zenit 3 SL (9%)
Option 6, 2 launches	**$C_3 = 0\ km^2/s^2$**	**3584 kg**	**Delta II (6%)** **Zenit 3 SL (11%)**
Option 7, 1 launch	$C_3 = 0\ km^2/s^2$	6649 kg	Delta IV (14%)
Option 7, 2 launches	$C_3 = 0\ km^2/s^2$	3314 kg	Delta II(13%)
Option 8, 4 launches	$C_3 = 0\ km^2/s^2$	1666 kg	Atlas II (17%) Sojuz (4%)

A summary of the results of the performed analyses in terms of total launch mass and available launchers mass margins is presented in Table 4, considering both one or more launches for each of the selected options, while the complete report of the quantitative analyses with detailed mass breakdowns can be found in the FSR.

In addition to the total launch mass, other two aspects have been considered for the trade-off: the lack of launch redundancy in case of single launch, that would lead to the total loss of the entire fleet of satellites in case of launcher failure, and the high mission operations complexity in case of separated transfers of the spacecrafts from Earth, that would lead to excessively high risks and costs. For these reason, all options involving single launch or separate transfers have been discarded; among the remaining alternatives, option 6 with two Zenith 3 SL launches, consisting of EP transfer with a propulsion module carrying 4 spacecrafts and of EP separate spiral-down, has been chosen in light of the lower mass. It has to be noted that the use of EP for both Earth–Mars transfer and Mars spiral-in implies a long time of flight, more than 4 years for the final trajectory, while CP would allow to reach the operational orbits in less than 1 year, but this aspect has not been considered critical in the frame of the studied robotic mission.

Following a more detailed mission analysis and subsystems design process (presented respectively in Sections 3 and 4) for both the spacecraft and the propulsion bus, the following baseline mission profile has been outlined:

1. Two Zenith 3 SL launches on a $C_3 = 0\ km^2/s^2$ escape orbit, each carrying an electric propulsion bus capable of delivering four satellites to Mars sphere of influence (SOI); selected launch date is for March 2021, but similar opportunities occur approximately every 2.19 years.
2. Low-thrust Earth–Mars 3.12 years transfer performed with the bus engines.
3. Mid-course low-thrust corrections tailored for the two buses with the purpose of reaching Mars SOI with the correct initial conditions for the assigned orbital plane.
4. Entrance in Mars SOI and spacecrafts separation from the buses, which get lost in space after an uncontrolled fly-by with a safe pericentre distance of more than 100,000 km from the planet.
5. Low-thrust spiral-in towards the operational orbits of the single electrically propelled spacecrafts; the dormant spare satellites reach a higher orbit at 18,250 km of altitude, that allows a faster re-deployment in case of failure of one of the active units.
6. Ten-years operational life in Mars orbit, acting as Earth pointers to allow the laser connection with Earth and contemporarily communicating with the users on Mars and with the other spacecrafts via the rotating antennas.
7. Constellation re-deployment in case of total failure of one of the satellites, with a worst-case time of 12 days for the full performance re-establishment.
8. End of life: transfer to a graveyard orbit 2000 km below the operational orbital planes, to avoid collisions with possible replacement units for another 10-years operational cycle.

3. Mission analysis

The mission analysis work has been focused on two goals, the computation of reference mission ΔV for all the studied transfer options with simplified models and, afterwards, the detailed study of the selected low-thrust Earth–Mars transfer and MOI.

For the first objective, both CP and EP transfers have been analyzed. For the impulsive scenario, the simple Lam-

bert problem has been solved obtaining a pork-chop graph for the total ΔV from GTO to the final operational orbit, considering aerobraking when it is advantageous with respect to the traditional MOI pericentre burn. Given the simplicity of this approach the results are not reported here and can be found in the FSR.

On the contrary, the EP scenario cannot be approached with simple computations, because the high number of variables influencing the low-thrust trajectory need to be optimized to obtain a minimum ΔV solution. Two different models have been developed for this purpose for the Earth–Mars transfer: first, a shape-based method based on the exponential sinusoids algorithm has been implemented, that provides estimations of the mission ΔV through fast optimization runs with few design variables, sufficiently accurate for the trade-off analysis; then, a more complex direct integration model with discretized control histories has been introduced to refine the final trajectory.

Both models and the related results are presented in the next two paragraphs, while Section 3.3 describes the approach followed for the Mars spiral-in phase, that results simpler in terms of number and type of variables.

3.1. Exponential sinusoids model for Earth–Mars trajectory preliminary design

The exponential sinusoids model used for the Earth–Mars trajectory preliminary design has been introduced by Petropoulos (2001) and then refined by Izzo (2006), and is a shape-based approach laying on the hypotheses of planar transfer and thrust always tangential to the velocity vector. As for classical Lambert's problem, the initial and final points of the trajectory are given by the position of the planets at the beginning and end of the flight, but its shape is defined by an exponential sinusoid; with the geometry of the transfer fixed, the acceleration profile can be reconstructed exploiting the equations of motion, thus providing an estimation of the required ΔV. It has however to be noted that only initial and final positions can be imposed as constraints, while the velocities at Earth and Mars are a consequence of the trajectory's shape. With this model, 4 parameters have been used as optimization variables: the launch date in the 2020–2030 timeframe, a TOF between 800 and 1500 days, the number of revolutions around the sun (from 1 to 5) and the exponential sinusoid shape parameter, $0.001 < k_2 < 1$, which describes how much the radius of the trajectory varies with the anomaly. A Matlab implementation of a state-of-art and widely used global optimization algorithm, the Non-dominated Sorting Genetic Algorithm-II (NSGA-II, described in Deb et al., 2000) has been used for a multi-objective optimization with the estimated ΔV and the relative velocity at Mars arrival as contrasting minimization objectives.

The best non-dominated front obtained after several runs of NSGA-II is reported in Fig. 5, showing the different transfer strategies that allow alternatively a lower transfer ΔV or a lower incoming velocity at Mars; from this

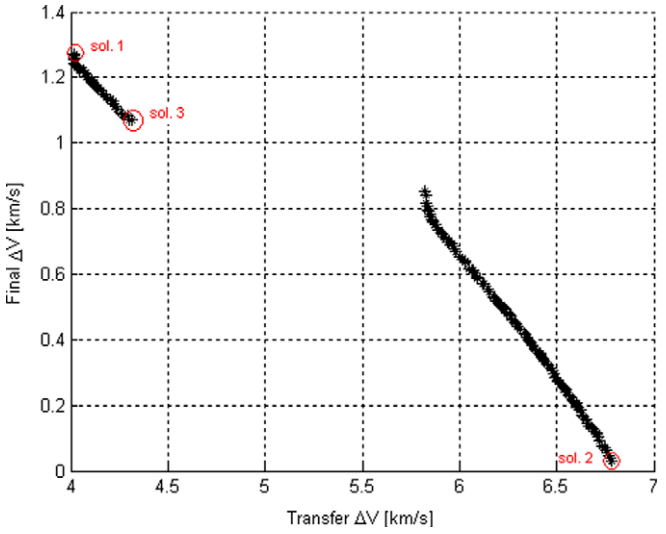

Fig. 5. Earth–Mars low-thrust transfer: Pareto-optimal solutions with respect to transfer and final ΔV, obtained with NSGA-II applied to exponential sinusoids model.

population of 150 individuals, 3 candidate transfer trajectories have been chosen for the system level trade-offs presented in Section 2.3: the minimum transfer ΔV (sol. 1) for option 4, which includes on-board CP engines for the MOI, the minimum arrival velocity (sol. 2) and the knee solution trajectory (sol. 3), both suitable for the EP only strategies (options 5, 6 and 7). From additional results, that are not shown here but can be found in the FSR, the minimum arrival velocity solutions has been discarded because of a too high required initial C_3 energy and an acceleration spike that doesn't allow an efficient dimensioning of the power system.

3.2. Direct integration model for Earth–Mars trajectory detailed design

Even though the exponential sinusoids method has provided valuable information with low computational effort for the initial trade-offs, it has been decided to develop a more complex direct integration model for later analyses, in light of two major disadvantages of the shape-based approach: first, the acceleration profiles always show a peak close to Mars, leading to an unacceptable inefficiency in the solar arrays sizing, and secondly the thrust direction is not included among the design variables, while a non-tangential thrust could improve the results in terms both of transfer and arrival ΔV.

In order to overcome these issues, a model has been implemented in Matlab/Simulink environment for the direct integration of the polar 2D equations of motion, while the inclination over the ecliptic of Mars orbit has been considered only in terms of definition of departure declination required to perform the Earth–Mars transfer on the right inclined plane.

In this model, the total time of flight is divided in 5 intervals of variable duration where the control parameters,

namely the acceleration level and the in-plane thrust angle, assume constant values. In addition to the launch date, the interval lengths, acceleration levels and thrust angles complete a set of 16 optimization variables; the objectives are still the transfer and final ΔV, but in this case the initial C_3 is set to 0, imposing a launch on a nearly parabolic escape trajectory.

The integration starts with a rough integration step of 10^6 s, necessary to keep the computational times within reasonable values, and then passes to an integration step of 10^3 s in order to provide higher definition when the spacecraft reaches the minimum distance of Mars orbit from the Sun. Hence, if the trajectory intersects Mars SOI the integration stops, returning a positive feedback. On the contrary if the maximum distance of Mars orbit from the Sun or a maximum TOF of 3.3 years is reached without intersecting the SOI, a negative feedback is returned and the optimization objectives are set to 10^6, in order to direct NSGA-II search towards different areas of the search space.

To force an acceleration profile with higher peaks closer to the Sun, higher upper boundaries of the acceleration levels have been defined for the first time intervals, whereas in order to allow ballistic arcs without adding more design variables, the acceleration level has been set to 0 if a given lower threshold is reached.

Fig. 6 shows the best non-dominated front obtained with the direct integration model, which is divided in 2 zones, the first with higher transfer ΔV and lower arrival ΔV, and the second with opposite characteristics. The selected highlighted solution, whose geometry is shown in Fig. 7 and whose main parameters are summarized in Table 5, has been chosen on the basis of system level considerations. The high Earth–Mars transfer ΔV has in fact imposed the use of gridded ion engines with high specific impulse for the propulsion module, whereas the high distance from the Sun in the Mars spiral-in phase has required the selection of Hall thrusters for the single spacecrafts, due to their much lower power consumption; for this reason, a strategy with a lower arrival ΔV, at the price of a higher transfer ΔV, allows to globally save propellant mass, since the specific impulse of Hall thrusters is significantly lower.

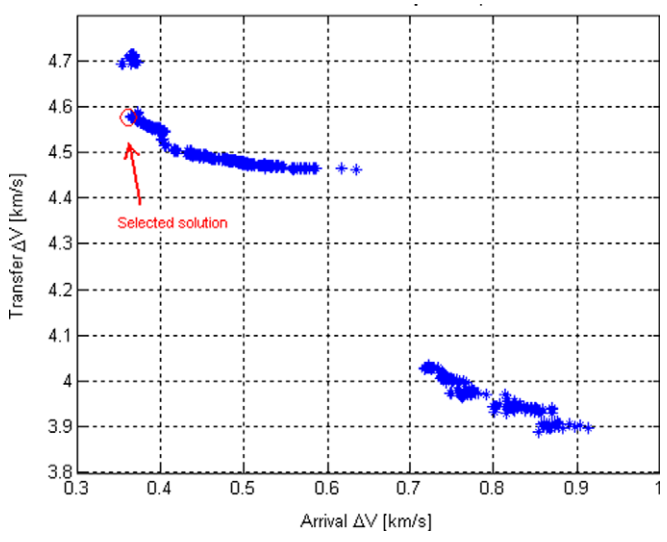

Fig. 6. Earth–Mars low-thrust transfer: Pareto-optimal solutions with respect to transfer and final ΔV obtained with NSGA-II applied to direct integration model.

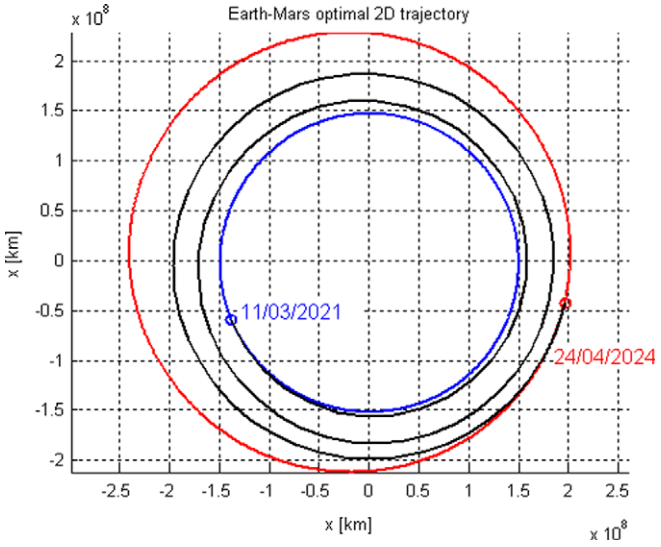

Fig. 7. Selected Pareto-optimal solution among those of Fig. 6: transfer trajectory geometry.

Table 5
Selected Pareto-optimal Earth–Mars transfer solution.

Launch date	11/03/2021	Launch C_3	0.066 km^2/s^2
Plane inclination*	−0.99°	δ_{EQ}**	−66°
δ_{ECL}***	−89.5°	Maximum thrust	0.22 N
TOF	3.12 years	Arrival in Mars SOI	24/04/2024
Transfer ΔV	4.552 km/s	Final ΔV	0.364 km/s

* Transfer plane inclination over the ecliptic.
** Launch declination with respect to equator.
*** Launch declination with respect to ecliptic.

It can be noted that the introduction of the direct integration model, though requiring longer computational times, has ensured a drastic improvement of the chosen optimal solution, which has almost the same transfer ΔV of the knee solution obtained with exponential sinusoids, but with a much lower relative velocity at Mars; moreover, the acceleration profile is such that the solar array area required as a function of the distance from the Sun is nearly flat, allowing an efficient design of the power system.

3.3. Mars spiral-in model

For the Mars spiral-in, a two-step trajectory design approach has been followed for the preliminary trade-off analysis and the successive detailed design phase. Since the purpose of this phase is to reduce the eccentricity of the incoming orbit from $e > 1$ to $e = 0$, a direct integration model has been employed with a constant and tangential thrust opposed to the direction of motion, switched on close to the pericentre and off near the apocentre. In fact,

an analysis of tangential perturbations in a two-body problem has shown that, by switching on the engine when $(\cos(\text{true anomaly}) + e) > 0$, the derivative of the eccentricity is always negative, leading to a continuous decrease of the apocentre height.

The model for the spiral-in is purely 2D, under the assumption that mid-course corrections can ensure the entrance in Mars SOI with the correct position and velocity vectors to obtain the desired orbital plane; the initial conditions for the integration are given at the planet's SOI with a velocity equal to 364 m/s, taken from the Earth–Mars selected Pareto-optimal solution. The pericentre radius of the incoming hyperbolic trajectory is thus the only free parameter, which has to be varied to get to the right final orbit within the given tolerances of 0.01 on eccentricity and 50 km on the semiaxis.

After several iterations of system design, the final wet and dry masses of the spacecrafts have been defined and a Hall effect engine with a maximum thrust of 50.9 mN has been chosen, capable of providing the required impulse for both orbital capture and a spiral-in phase towards the operational orbit within the constraint of a maximum TOF of one year.

The final spiral-in trajectory is shown in Fig. 8, with the propelled phases in a different colour, and its main parameters are summarized in Table 6, showing a total ΔV of around 1 km/s allowing to embark less than 40 kg of xenon propellant and resulting in 4.1 years of travel from launch to the operational phase.

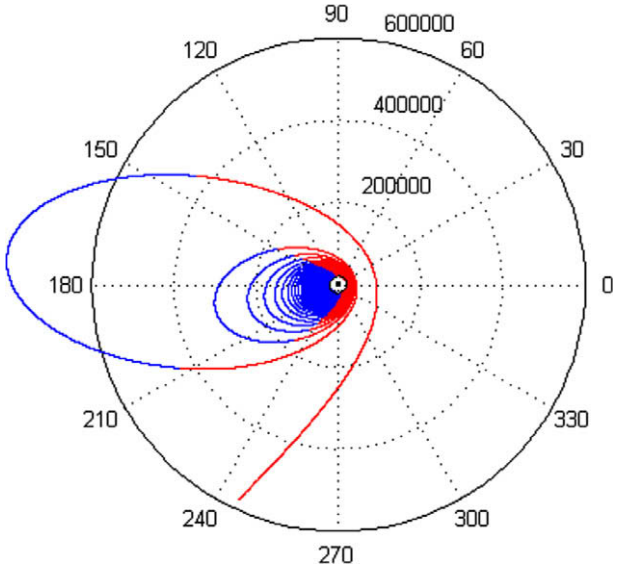

Fig. 8. Mars spiral-in results for the final spacecrafts configuration: optimal trajectory geometry. Propelled phases close to the pericentres are in red. (For interpretation of color mentioned in this figure the reader is referred to the web version of the article.)

4. System review

After a design process consisting of several iterations of subsystems sizing, which has reached a rather high level of detail for a feasibility study, the system design has been frozen for both the satellites of the constellation and the propulsion buses carrying them to Mars. The final results of the process are summarized in this section, whereas the FSR contains a more detailed description of each subsystem.

It has to be preliminarily noted that the propulsion buses can be considered as full-fledged spacecrafts, even though with simplified design since some of the functions are carried out by the single satellites. All functionalities that can be performed by the satellites subsystems have in fact not been duplicated on the bus, allowing significant mass savings, specifically communications with Earth and most of the attitude control and power generation functions during cruise phase. For this reason the bus and the satellites are linked together not only mechanically but also through power and data wiring, that allow the energy transfer from the satellites solar arrays to the bus electrical engines, as well as the exchange of information between the satellites processors and the bus subsystems (e.g. engines commands uploads).

The constellation satellites in deployed configuration and the bus external layout are shown in Figs. 9 and 10; the laser telescope, the lower antennas mechanism and an upper secondary antenna are clearly visible in the spacecraft, whereas the geometric dimensions are reported for the bus in stowed configuration; after release from the launcher, one solar array deployed from each spacecraft (the other is on the side attached to the bus) and two additional arrays on the lower section provide the almost 10 kW necessary for the survival of the spacecrafts and the EP engines. Summarized system level mass budgets are presented in Tables 7 and 8 for the spacecraft and the bus; margins are taken at component level, that are not shown in the tables but can be found in the detailed mass breakdown of the FSR, as well as subsystem and system level, with a total launch mass of 3587 kg resulting from the design process, 11.3% less than the maximum mass that can be injected into the escape orbit by the selected Zenith 3 SL launcher.

A preliminary cost analysis has also been performed; the space segment and mission operations costs for the 8 satellites and the 2 propulsion buses, obtained with parametric

Table 6
Mars spiral-in results for the final spacecrafts configuration: optimal trajectory main parameters.

Incoming orbit $H_{Peric.}$	104,900 km	Maximum acceleration	1.04×10^{-4} m/s^2
Mars SOI entrance	24/04/2024	Operative orbit insertion	18/04/2025
TOF	359.4 days	Total transfer time from launch to final orbit	4.1 years
Spiral-in ΔV	1.027 km/s	Time with the engine on	2971.9 h

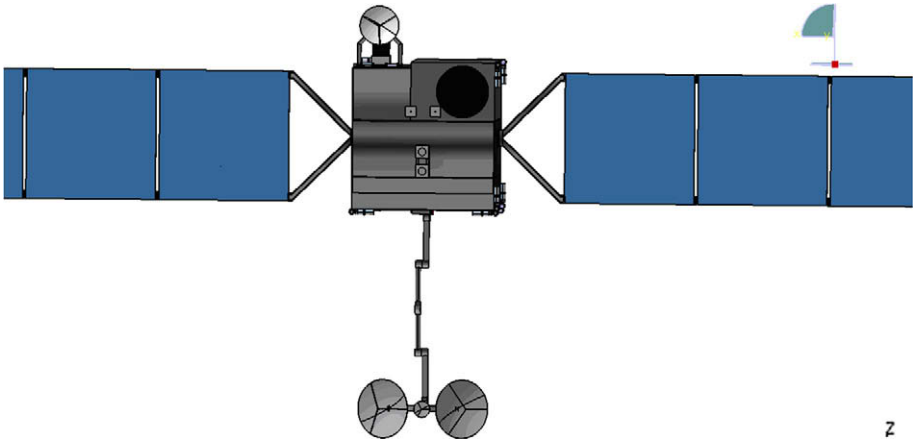

Fig. 9. Constellation satellite in operational configuration, with deployed solar arrays and lower antennas, mounted on the 3-DoF mechanism; clearly visible in the front face are the telescope in the upper right part and the two Hall thrusters in the centre; the secondary X-band antenna for the transfer phase is placed on the top.

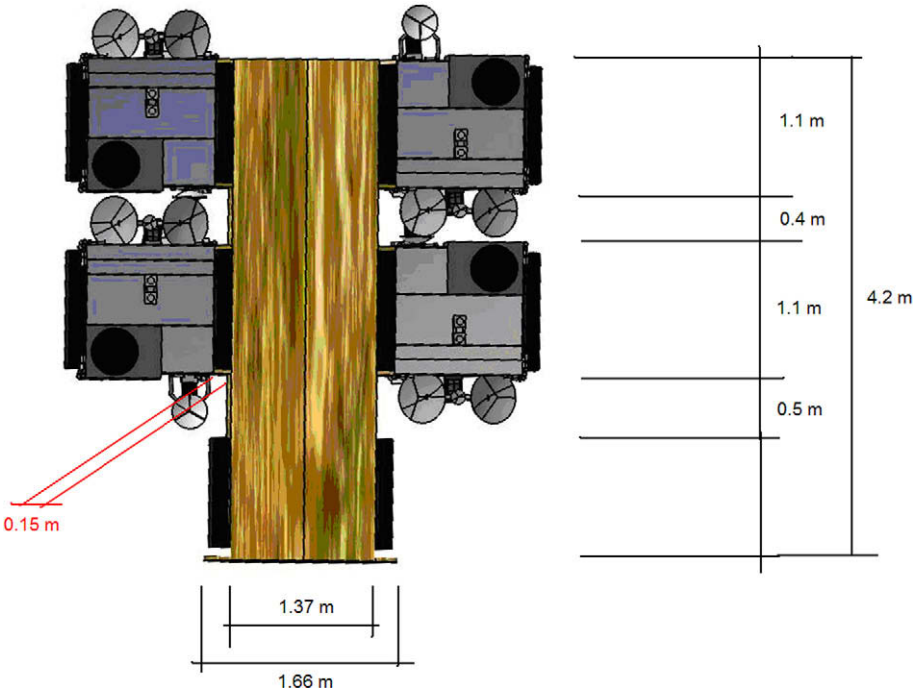

Fig. 10. Propulsion bus configuration with 4 attached spacecrafts; one 8-m long solar array is deployed from each spacecraft and additional two 10-m arrays are deployed from the bottom section; the faces visible from this perspective are always directed towards the Sun to provide power, while radiators are on the back side and ion engines are directed downwards.

cost estimation relationships from the Small Satellite Cost Model (Lao et al., 1998), have been added to the laser payloads and ground stations cost suggested by Hemmati (2005) and to the Zenit 3 SL commercial launch cost, totalling around 800 FY2005 M€ with a estimated uncertainty of the 40%.

4.1. TT&C and ADCS

The Telemetry, Tracking and Control (TT&C) subsystem represents the main payload of the mission, and the entire satellites design has been developed around it; the propulsion buses on the contrary do not include any communication device, and both telemetry download and commands upload occur through the satellites systems.

The communication subsystem on-board each spacecraft can be divided in two part, the laser devices for Earth–Mars link and the RF chain for communications with the surface and inter-satellite links. Additionally, an auxiliary small X-band directional antenna has been fitted into the configuration in order to ensure communications with Earth during the Earth–Mars transfer. For volume constraints in fact, the antennas mounted on the 3-DoF mechanism can be deployed only after separation from

Table 7
Final mass budget for each spacecraft of the constellation, divided by subsystem and showing margins.

	Mass [kg]	Margin	Margined mass [kg]
TT&C	67.93	0.10	74.7
OBDH	14.65	0.10	15.3
TCS	10.00	0.10	11.0
Propulsion	37.30	0.10	41.0
EPS	110.29	0.10	121.3
ADCS	26.90	0.20	32.3
Stru. & Mech.	130.39	0.00	130.4
Harness	18.00	0.25	22.5
Total system dry	448.0	10.0	**492.8**
Propellant	32.70	0.15	37.6
Total system wet			**530.4**

Table 8
Final mass budget for each propulsion bus, divided by subsystem and showing margins.

	Mass [kg]	Margin	Margined mass [kg]
TT&C	0.00	0.10	0.00
OBDH	9.12	0.10	10.0
TCS	45.00	0.10	49.5
Propulsion	104.60	0.10	114.9
EPS	121.88	0.10	134.1
ADCS	30.19	0.20	36.2
Stru. & Mech.	625.40	0.00	625.4
Harness	24.16	0.25	30.2
Total bus dry	999.21	10.0	**1091.4**
Bus dry + 4 satellites wet			**3220.7**
Propellant	278.40	0.10	306.2
Total launch mass	(including 60 kg of adapter)		**3586.9**
Launcher capacity	**4005.0 kg**	**Launcher margin**	**11.3%**

the bus, and serve as primary Earth–Mars communication system only during Mars spiral-in.

The optical communications architecture consists in a transmitter and a receiver, the former based on laser emission and the latter on photons counter, while the data coding is performed through Pulse Position Modulation (PPM). The optical assembly developed at Lincoln Labs/MIT, under the direction of Goddard Space Flight Center (GSFC), for the MTO program is shown in Fig. 11 (JPL, 2003, p. 26) and has been chosen for this mission; it consists of two cold redundant laser sources maintained for thermal reasons far from the optics of a 30 cm telescope.

It has to be noted that the main challenge associated to the use of optical links for deep space communications is represented by the highly fine pointing requirements of the laser device. The laser beam is in fact so narrow that its spot on Earth at the maximum Earth–Mars distance of 2.7 AU is in the order of few thousands km of diameter, therefore requiring pointing accuracies in the order of the μrad. Such a precision is not achievable with current state-of-art Attitude Determination and Control Systems (ADCS), therefore it has to be ensured by fine optics pointing devices, while the satellite platform is maintained three-axis stabilized with the telescope axis aligned with the Earth direction with a much lower accuracy of 0.05°; a traditional ADCS has been designed to fulfil this rather simple requirement, composed of 2 star trackers for the fine attitude determination, 2 sun sensors for coarse attitude acquisition and solar arrays pointing, 4 reaction wheels for disturbance torques compensation and slew manoeuvres and 24 hydrazine thrusters for the wheels de-saturation and contingency manoeuvres. Additionally, 4 reaction wheels are designed to be mounted for redundancy on the propulsion buses for manoeuvres and disturbances compensation during the Earth–Mars transfer, while the attitude control main functions are left to the single spacecrafts even in this phase.

The same LL/MIT optical assembly mentioned above also incorporates the optics pointing mechanisms (described by Lee et al., 2001; Townes et al., 2004) and a Magneto-hydrodynamic Inertial reference Unit (MIRU, Laughlin et al., 2002) that ensures the highly precise

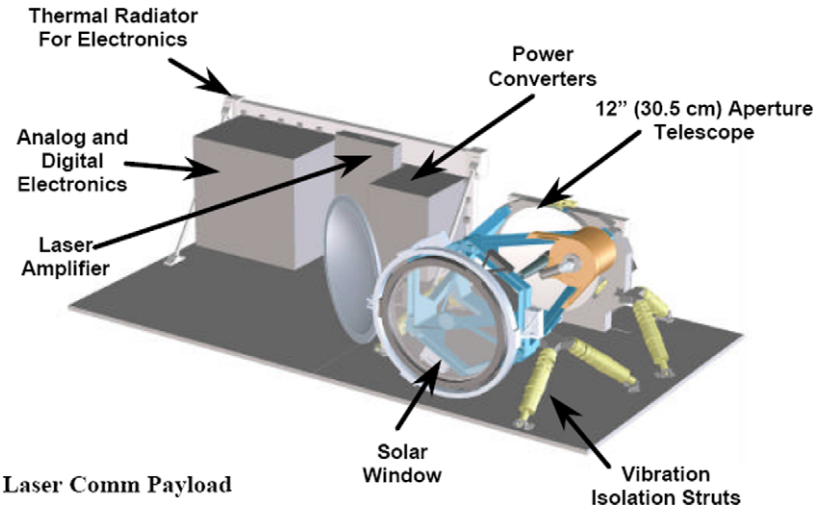

Fig. 11. Schematic view of the optical assembly developed at LL/MIT for the MTO program.

angular motion measurement needed for the fine pointing control. The main issue related to the proposed laser assembly is the extreme thermal stability required, within 4°, that is ensured by a cold-biased thermal control system with close loop control of the laser through thermostats and heaters. The redundancy of the system is limited to the laser sources, but its total loss on-board one or even two satellites per orbital plane, as explained in Section 2.2, has a limited effect on the constellation performance since the communication towards Earth can be relayed by the other active satellites or by the dormant spare.

For the RF communications on the contrary, two traditional X-band and Ka-band chains have been designed, with redundancies on the amplifiers and on the newest generation transponders, the Small Deep Space Transponder (SDST) recently validated at JPL (Chen et al., 2004). The lateral 45 cm Ka antennas and the central 12.5 cm X antenna are mounted at the bottom of the 3-DoF mechanisms shown in Fig. 9.

Lasercom link budgets have been performed mainly on the basis of data published by Biswas and Piazzolla (2003), as well as traditional RF link budgets for different scenarios, and their detailed description can be found in the FSR; among the others, the maximum Earth–Mars distance up and downlink, the inter-satellite link and the constellation-to-surface communication involving a possible human base with a 2 m antenna, have worst-case data-rates of 13.7 Mbps, 10.2 Mbps, 4.8 Mbps and 4.3 Mbps, as summarized in Fig. 1, with power consumption of 99 W for the laser, 45 W for the Ka-band and 73 W for the X-band. The developed communication architecture, though rather complicated, is therefore able to accomplish its mission with a sensibly higher performance with respect to the minimum imposed requirement.

As a final remark, it has to be noted that the ground segment for deep space communications is a relevant aspect with respect to the total mission costs. The use of relay satellites in Earth orbit has been investigated, but it has not been deemed necessary because the atmospheric attenuation is very low at the selected wavelength of 1064 nm. During the past few years two different ideas have instead been proposed for the optical network, consisting either of few standard antennas, with a diameter of 10–12 m each, or of an array of 80 small antennas of 1 m of diameter each, that according to Khaltri et al. (2004) would allow an additional increase in the data-rate; however, the more traditional first option has been selected, defining a ground segment consisting of seven antennas of 12 m of diameter, with locations optimized for the narrow spot of the laser beam, that would have to be specifically built for this mission. However, a detailed study reported in Hemmati (2005) states that the implementation of an optical network would be more convenient than the further improvement of the current X/Ka-band ground stations if the number of missions taking advantage of it becomes larger than 5–6.

4.2. Propulsion and EPS

The choice of EP leads to important system level considerations, first of all the substantial increase in the power demand, due to the engines high power consumption, and the strong coupling of the propulsion and Electrical and Power System (EPS), requiring several design iterations to converge to a consistent solution.

The main trade-off to be performed for the propulsion system is between gridded ion engines, that provide higher specific impulses, and Hall effect thrusters, that have the advantage of a much lower power demand. The choice has been performed at system level as shown in Section 2.3, including in the loop EPS, propulsion and mission analysis disciplines, and has resulted in the selection of the BHT-1000 Hall effect thruster for the single spacecrafts, providing the required 50.9 mN of constant thrust with 830 W of power demand and 1750 s of specific impulse, and of the RIT-22 gridded ion engine for the propulsion buses, capable of a thrust range of 50–250 mN that is very well suited for the required thrust profile, varying between 220 and 150 mN during the Earth–Mars transfer. Fig. 12 reports mass, power and specific impulse profiles for the transfer, showing the coast phase defined by the mission analysis optimization and the decrease of thrust, and thus of required power, enforced to compensate the diminishing power provided by the solar arrays as the bus spirals out towards Mars.

It has to be noted that one of the current limitations of EP systems is the short lifetime due to the engine erosion caused by the high velocity electrons; for this reason, although the propelled phases lengths provided by the mission analysis are within the theoretical lifetimes of the selected engines, a redundant thruster has been included in the design of both the propulsion buses and of the constellation satellites, mounted on a mechanism that allows its orientation along the longitudinal axis in case of failure of the primary thruster.

As regards to the spacecrafts EPS, the power budget indicates that the propelled spiral-in phases, requiring 1.4 kW of power including margins, define the sizing of the two deployable solar arrays, resulting in 8 panels each at a 28% BOL efficiency for a total area of 16 m^2. For Earth–Mars transfer as well, the bus solar arrays are sized at Mars, even though the excess power closer to Earth is low due to the increased thrust level; the total power request at Mars is thus of 7.9 kW, including margins and the power needed for the 4 carried spacecrafts, that can be satisfied by the 4 arrays of the spacecrafts that can be deployed from the beginning of the flight plus additional 2 larger arrays mounted on the bus, for a total of 52 m^2; the peak power provided by such an array at Earth distance is of almost 10 kW.

It has to be noted that the power generated by the spacecrafts in the final Mars orbit is much higher than the power requested for the nominal operations; this power surplus (577 W after 10 years and at the maximum distance of

Mars from the Sun) can both be considered as a redundancy or exploited to provide power for secondary scientific payloads to be added to the current design.

For the complete description of both the propulsion and the EPS systems dimensioning, refer to the FSR.

4.3. TCS, OBDH and Structures

The Thermal Control System (TCS), On-Board Data Handling (OBDH) and Structures subsystems do not present particular issues, resulting in a rather traditional design.

For the TCS, several cases have been analyzed in order to define the worst conditions, and a cold-biased design has been selected, composed of sensors, heaters and radiators thermal blankets as only TCS components; for the spacecrafts, the worst-case hot is represented by those periods of the spiral-in phase with the main radiator facing the direct Sun light (such a condition cannot be avoided due to the pointing requirements of thruster and solar arrays), while the worst-case cold occurs at the arrival at Mars SOI, still far from the radiative source of Mars. From the node model analyses, a final configuration with a main radiator of 0.5 m^2 and two lateral radiators of 0.125 m^2 has been selected, requiring 198 W of 10% margined heaters power in the worst-case cold.

It has to be noted that the electrical engines dissipate a large quantity of power, therefore they can both represent a resource and an issue in the design of a TCS. The BHT-1000 engines, with a low 52% power efficiency, have been placed outside of the spacecrafts, in order to avoid the radiators oversizing, whereas the more efficient RIT-22 engines (81%) have been housed inside the propulsion buses to reduce the amount of heating power needed at the Mars SOI. Moreover, to overcome the too low heat conduction in the sandwich plates of the structure, the honeycomb has been designed to be filled with a thermal conductive foam that allows to manage the cold case with 517 W of

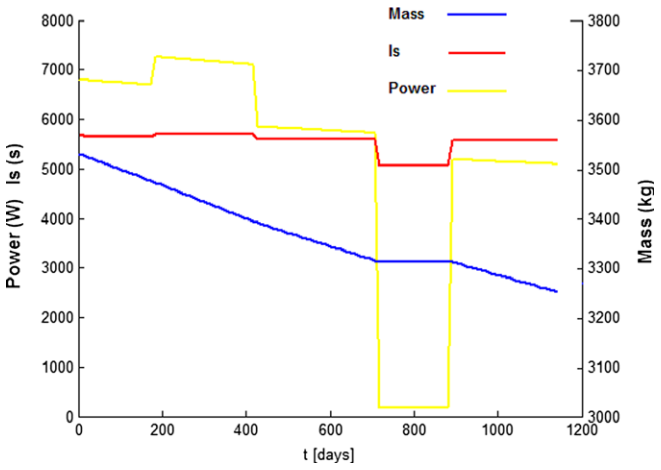

Fig. 12. Power, specific impulse and propellant mass profiles for the RIT-22 gridded ion engine along the selected Earth–Mars optimal transfer trajectory.

margined heaters power, while the hot case at Earth is dealt with two radiators of 0.9 m^2 and 2.4 m^2, placed on the face always directed towards the empty space, aimed at ensuring the thermal dissipation respectively for the upper section with the attached spacecrafts and the lower section with solar arrays, electronics and propulsion system.

For the OBDH of the satellites, the sizing requirement is the high communications data-rate to be dealt with during the operational phase, that has been estimated in 40 m^2Mbps including laser and RF up and downlink, and margined to 80 Mbps to take into account possible advances in communication technologies; this leads to an approximate throughput of 600 Mega Instructions Per Second (MIPS). Two cold redundant on-board computers with a maximum throughput of 1800 MIPS have therefore been selected, with a power consumption of 10 W at 600 MIPS and a sustainable radiation dose of more than 10 krads; since estimates foresee a total of 1.3 krads during the entire lifetime, the hardware casing has been designed to be a thin 2 mm aluminium box. The overall system design includes additional cards for the interfaces with the laser and RF payloads and the power management unit, leading to total margined 16.1 kg and 30.7 W to be allocated for the OBDH. The same OBDH architecture has been selected for the buses, even though over-dimensioned for the propulsion and power functions management, in order to decrease the development costs.

The spacecrafts and propulsion bus structures have been dimensioned considering the envelop of Ariane 5 and Zenith 3 SL launch loads, in order to maintain a back-up launch solution with the European launcher. The bus structure, whose finite element model (FEM) is shown in Fig. 13, is composed of longitudinal thin elements panelled all around and reinforced with transverse wing-ribs as an aeronautical beam; additional elements are the base-ring bolted to the launcher adaptor of 1664 mm of diameter, and the reinforced arms used to connect the spacecrafts with the bus structure. With Al 2024 T3 material both for the beams and the sandwich panels, the structure totals 605 kg with a 10% margin and is able to sustain the launch loads including safety factors, with first lateral and axial frequencies of 11.8 Hz and 33.7 Hz, both compatible with the selected launchers.

A FEM has been developed for the satellites as well, composed of aluminium sandwich plate elements reinforced on the side attached to the bus, and the final design foresees a total of 71.5 kg for both the primary and secondary elements of the structure, allowing to survive the launch environment and showing a first natural frequency at 45.9 Hz.

5. Final remarks and scientific opportunities

The paper has presented a feasibility study for the set-up of a communication constellation around Mars with the purpose of supporting massive robotic scientific exploration and the first human missions in the 2025–2035 timeframe; after

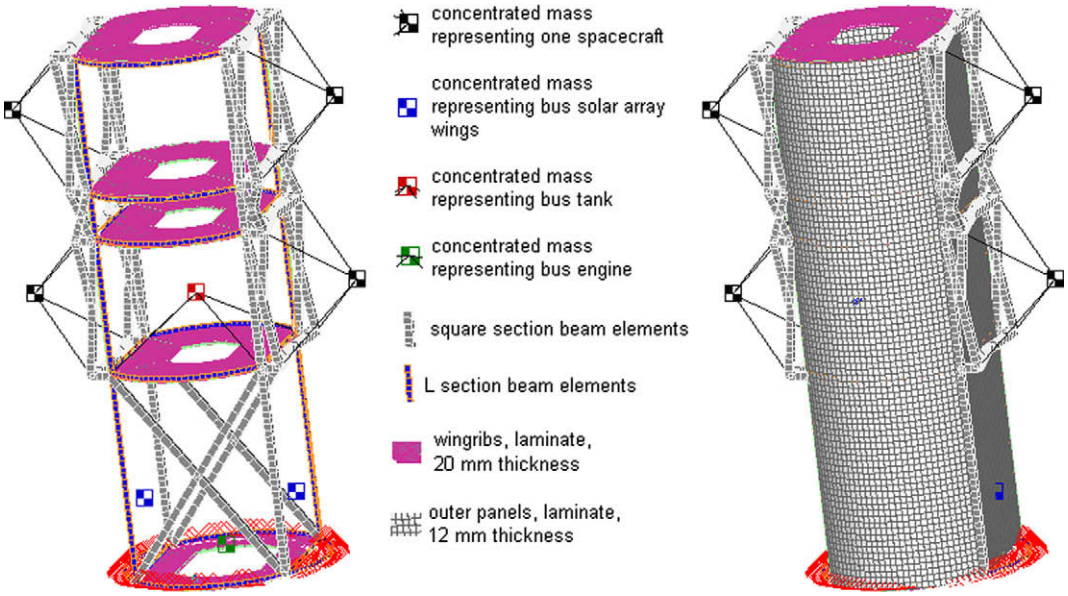

Fig. 13. FE model of the propulsion bus structure. Note the reinforced connections to the 4 carried spacecrafts.

quantitative trade-offs regarding communication technology and architecture, constellation configuration and transfer strategy and a rather detailed design process, a baseline mission design has been outlined that fully satisfies the tough requirement of continuous coverage of the entire Mars surface, with a worst-case Mars–Earth data-rate of more than 10 Mbps and a triple system redundancy. Moreover, although the simplified cost estimation employed at this stage has high uncertainty, the resulting reference cost of 800 FY2005 M€ for the entire program seems affordable in the context of an international effort in the order of hundreds of billions of dollars for Mars human exploration.

The main challenges of the proposed mission are represented by the management of the operations of a constellation of 8 satellites around Mars, and by the TRL enhancement of the laser technology for long range communications; it has to be noted that the latter issue, requiring the solution of complicated technical problems as the strict pointing requirements and the allocation of significant funding for the build-up of several optical ground stations, could cause delays in the implementation of the project, that nevertheless already foresees a very optimistic launch date with respect to the currently most probable 2030–2040 timeframe for the first Mars human flight; besides, the development of an optical communications infrastructure would lead to an important technological jump for all planetary exploration, allowing to achieve high data-rates till now unthinkable for deep space missions.

As a final remark, the set-up of a Mars constellation would have the important side effect of providing the opportunity for the contemporary observation of the planet from many orbiting platforms with the same design, therefore capable of embarking the same complement of scientific instruments; for instance, global circulation and climatological cycles, the atmospheric vertical structure variations or the condensation clouds temporal distribution represent fields of study that would strongly benefit from such availability. As shown in the paper, the current design foresees 105 kg and 577 W of mass and power margins for each satellite in the constellation; of course, the introduction of additional instruments would imply a partial redesign of the spacecraft, resulting in some of the resources being allocated for additional fuel, transmission power or similar needs, but the available mass and power largely exceed the requirements of typical planetary science instruments (e.g. Mars Climate Sounder, MCS, on-board MRO needs 9 kg and 11 W and is able to perform remote sensing of the vertical structure of atmospheric pressure, temperature, dust and water content with high spatial resolution).

As an alternative, the most effective network science architecture would be the set-up of several surface stations associated with at least one orbiting sounder, that would also allow to investigate other aspects from the ground, such as Mars seismology and internal structure, or the planetary boundary layer and surface-atmosphere interactions. According to Harri et al. (2007), the feasibility study for the Met-Net mission, in the frame of ESA Cosmic Vision program, has led to the conceptual design of small passively controlled 30-kg scientific probes with an innovative hard landing system, to be separately targeted during the interplanetary journey directly from a carrying spacecraft to reach different locations on the surface of Mars. If such a mission will not be implemented separately in the upcoming years, it appears feasible to include up to 6–8 of these probes on each of the propulsion buses, and to slightly modify the two spare satellites to carry an MCS-like instrument for the orbital sounding, also providing them with a primary mission before any failure occurs. The merging of the communication mission proposed in this paper with a network science infrastructure would in this way give the unique opportunity of obtaining important results and possibly new discoveries about Mars

environment and history, and to contemporarily pave the way for the human arrival on the Red Planet.

Acknowledgments

The authors would like to acknowledge the other components of the students team: Alessandro Baronio (jimbelow@gmail.com) for the ADCS, Mauro Bartesaghi (mauro.bartesaghi@gmail.com) for the EPS, Marcello Gianguzzi (m.gianguzzi@alice.it) for the TCS, and Gabriele Greco (gabrielegreco1983@libero.it) for the propulsion system.

Appendix A.

Acronyms and abbreviations

ADCS	Attitude determination and control system
AU	Astronomic unit
BOL	Beginning of life
DoF	Degree of freedom
DSN	Deep space network
EOL	End of life
EPS	Electrical and power system
FEM	Finite elements model
FSR	Final study report
Fiscal Year 2005,	FY2005 M€ millions of Euros
GTO	Geostationary transfer orbit
JPL	Jet propulsion laboratory
Kbps	Kilobits per second
OBDH	On-board data handling
Mbps	Megabits per second
MCS	Mars climate sounder
MGS	Mars global surveyor
MIPS	Mega instructions per second
MIRU	Magneto-hydrodynamic inertial reference unit
MOI	Mars orbit insertion
MRO	Mars reconnaissance Orbiter
MSR	Mars sample return
MTO	Mars telecom orbiter
SL	Sea launch
SOI	Sphere of influence
RAAN	Right ascension of ascending node
R&D	Research and development
RF	Radio frequency
SDST	Small deep space transponder
TCS	Thermal control system
TOF	Time of flight
TT&C	Telemetry tracking and control

References

Biswas, A., Piazzolla, S. Deep-space optical communications downlink budget from Mars: system parameters. The Interplanetary Network (IPN) Progress Report 42-154. Published by Jet Propulsion Laboratory, August 15, 2003.

Biswas, A., Piazzolla, S. Deep-space optical communications link availability and data volume. The Interplanetary Network (IPN) Progress Report 42-162. Published by Jet Propulsion Laboratory, August 15, 2005.

Cesarone, R., Hastrup, R.C., Srinivasan, J., Morabito, D. Mars comm/nav microsat network. In: Proceedings of the 13th AIAA/USU Conference on Small Satellites, SSC99-VII-5, Utah State University, August 1999.

Chen, C.C., Shambayati, S., Makowsky, A., et al. Small Deep Space Transponder (SDST), DS1 Technology Validation Report. Jet Propulsion Laboratory, 2004.

Deb, K., Agrawal, S., Pratap, A., Meyarivan ,T. A fast elitist non-dominated sorting genetic algorithm for Multi-Objective Optimization: NSGA-II. In: Proceedings of the Parallel Problem Solving from Nature VI Conference, Springer, pp. 849–858, 2000.

Gangale, T., Byford, D., Goppert, J. Optimal Location of Relay Satellites for Continuous Communication with Mars, AIAA paper 2008-7919, 2008.

Harri, A.M., Leinonen, J., Merikallio, S. et al. MetNet – in situ observational network and orbital platform to investigate the Martian environment. Finnish Meteorological Institute Report 2007.3, 2007.

Hemmati, H., Layland, J., Lesh, J., et al. Comparative study of optical and RF communication systems for a Mars mission. In: Proceedings of SPIE, vol. 2699, Free-Space Laser Communication Technologies VIII, San Jose, California, pp.146–164, 1996.

Hemmati, H., Layland, J., Lesh, J., et al. Comparative study of optical and RF communication systems for a deep-space mission. The Telecommunications and Data Acquisition (TDA) Progress Report 42-128. Published by Jet Propulsion Laboratory, February 15, 1997.

Hemmati, H. Deep space optical communications. In: Hemmati, H. (Ed.), Jet Propulsion Laboratory-Caltech, Deep Space Communications And Navigation Series, October 2005.

Izzo, D. Lambert's problem for exponential sinusoids. Journal of Guidance, Control and Dynamics 29 (5), 1242–1245, 2006.

Jet Propulsion Laboratory. Mars Telecom Orbiter: Spacecraft Design Study, Mission and Payload Description Requirements, and Constraints, NASA JPL Request for Proposal No. 62503, June 2003.

Khaltri, F.I., Boroson, D.M., Murphy, D.V., et al. Link analysis of Mars–Earth optical communications system. In: Proceedings of SPIE, vol. 5338, Free-Space Laser Communication Technologies XVI, San Jose, California, pp. 143–150, January 2004.

Lao, N.Y., Mosher, T.J., Neff, J.M, Small Satellite Cost Model Version 98, User's Guide, Aerospace Corporation, Los Angeles, California, June 1998.

Laughlin, D., Sebesta, H., Eckelkamp-Baker, D. A dual function magneto-hydrodynamic (MHD) device for angular motion measurement and control. In: 25th Annual AAS Guidance and Control Conference, AAS-02-061, Breckenridge, Colorado, February 2002.

Lee, S., Alexander, J.W., Ortiz, G.G. Sub micro-radian pointing system design for deep-space optical communications. In: Proceedings of SPIE, vol. 4272, Free-Space Laser Communication Technologies XIII, San Jose, California, pp. 104–111, January 2001.

Moision, B., Hamkins, J. Deep-space optical communications downlink budget: modulation and coding. The Interplanetary Network (IPN) Progress Report 42-154. Published by Jet Propulsion Laboratory, August 15, 2003.

Morabito, D., Hastrup, R. Communications with mars during periods of solar conjunction: initial study results. The Interplanetary Network (IPN) Progress Report 42-147. Published by Jet Propulsion Laboratory, August 15, 2001.

Petropoulos, A.E. Shape-based approach to automated, low-thrust, gravity-assist trajectory design. PhD Thesis. School of Aeronautics and Astronautics, Purdue University, West Lafayette, Indiana, 2001.

Strizzi, J.D., Kutrieb, J., Damphousse, P., Carrico, J. Sun-Mars libration points and Mars mission simulations, AAS-01-159, AAS/AIAA Spaceflight Mechanics 2001. Advances in the Astronautical Sciences 18 (February), 807–822, 2001.

Townes, S.A., Edwards, B.L., Biswas, A., et al. The Mars laser communication demonstration, 2004. In: IEEE Aerospace Conference Proceedings, vol. 2, pp. 1180–1195, March 2004.